Enhanced trapping of cold ^{6}Li using multiple-sideband cooling in a two-dimensional magneto-optical trap

Kai Li,[1] Dongfang Zhang,[1] Tianyou Gao,[1] Shi-Guo Peng,[1] and Kaijun Jiang[1,2,*]

[1]*State Key Laboratory of Magnetic Resonance and Atomic and Molecular Physics, Wuhan Institute of Physics and Mathematics, Chinese Academy of Sciences, Wuhan, 430071, China*

[2]*Center for Cold Atom Physics, Chinese Academy of Sciences, Wuhan, 430071, China*

(Received 13 May 2015; published 22 July 2015)

Trapping a large number of ^{6}Li atoms in a simplified experimental setup is a long-term pursuit in the studies of degenerate Fermi gases. We experimentally and theoretically demonstrate the enhancement of ^{6}Li trapping efficiency in a three-dimensional magneto-optical trap (3D MOT) by using the multiple-sideband cooling in a two-dimensional magneto-optical trap (2D MOT). In the 2D MOT, we increase the spectral width of the cooling light to 102 MHz by generating six frequency sidebands in order to couple fast atoms. The capture velocity is dramatically increased by employing the multiple-sideband cooling. The number of trapped atoms in the 3D MOT is 6.0×10^8, which is higher by a factor of 4 than in the case of single-frequency cooling. We have investigated the dependence of atom number on laser detuning, and our experimental result agrees well with the prediction of a simple two-level model. The efficiency of the multiple-sideband cooling for lithium (in contrast to many other alkali-metal atoms) is also confirmed by the analysis of the loss due to fine-structure changing collisions.

DOI: 10.1103/PhysRevA.92.013419 PACS number(s): 37.10.−x, 37.20.+j, 67.85.−d

I. INTRODUCTION

Laser cooling and trapping [1,2] is the first step to set up a cold atom laboratory in which one can carry on a wide range of research, such as atomic interferometry [3], high precision atomic clocks [4,5], precise spectroscopy [6], quantum simulation [7], and ultracold chemistry [8,9]. In this context, quantum degenerate Fermi gases have a prospective research potential due to their long lifetime in the strong interaction regime and tunability of the atomic interactions [10]. This allows a reachable tabletop to study the equation of state of strongly interacting Fermi gases [11,12], fermionic polaron behavior [13,14], spin-orbit coupling effect [15,16], and anisotropic character of p-wave or higher partial wave interactions [17,18]. Due to the presence of a wide Feshbach resonance (∼300 G) [10,19], ^{6}Li can be extensively studied in the regime of quantum degeneracy. Therefore, obtaining a large number of trapped atoms is an important goal [20].

However, building up a simplified experimental setup to get a large number of trapped lithium atoms is still an open problem. First of all, due to a high melting temperature (∼454 K), a large number of Li atoms can be initially created only at very high temperatures (∼600 K). Therefore, cooling and trapping of Li initially employed the Zeeman-slower configuration [21,22], where fast-moving atoms were first slowed by resonant lasers with the help of magnet induced frequency shift and then loaded in a regular magneto-optical trap (MOT). In this case, one could trap $\sim 10^9$ atoms [20], but substantial efforts were required to complete the system design and construction, mostly because of complexity of magnetic coils and big volume of the vacuum chamber.

In the past decades several research groups have tried various methods of improving lithium loading in a simplified setup. Madison and colleagues collected lithium from a vapor chamber, where they could trap $\sim 10^7$ atoms [23]. In their experiment an atomic oven was placed close to the trapping region to reduce losses due to transverse divergence, and an atomic block was set in the center to avoid losses of trapped atoms induced by their collisions with high-speed ones. Kasevich's group applied a comb-frequency laser to directly load lithium in a vapor chamber where the broadened spectrum (∼125 MHz) could increase the capture velocity and then couple faster atoms. They also got $\sim 10^7$ atoms [24]. However, when atoms were directly loaded from the vapor cell as in Refs. [23,24], the number of trapped atoms was limited because of a small fraction of low-velocity atoms in the flux arriving at the trapping region. Walraven and colleagues applied a two-dimensional MOT (2D MOT) as the first cooling step and then pushed the slowed atoms to the three-dimensional (3D) trapping region [25]. Using this method they achieved an atom number which was comparable to that in the Zeeman-slower configuration.

In this paper we use the multiple-sideband cooling in a two-dimensional magneto-optical trap (2D MOT) to improve the ^{6}Li atoms trapping. We first employ multiple-sideband cooling with a spectral width of 102 MHz to slow fast-moving atoms in the 2D MOT, and then push the cooled atoms with a resonant laser beam to the 3D MOT. The atom number in the 3D MOT is 6.0×10^8, i.e., it is increased by a factor of 4 for our same apparatus over the case where we use a single cooling frequency with optimized detuning. We also measure the dependence of the atom number on laser detuning, where a theoretical prediction based on a simple two-level model has an agreement with the experimental results. The proposal demonstrated in this paper has the following advantages: (i) the multiple-sideband cooling can increase the number of trapped atoms compared to that in the single-frequency cooling; (ii) the 2D cooling stage can simplify the experimental setup compared to that in the Zeeman-slower configuration; (iii) our cooling method may be used for other species which cannot be directly loaded from a vapor chamber. The enhancement of the

*kjjiang@wipm.ac.cn

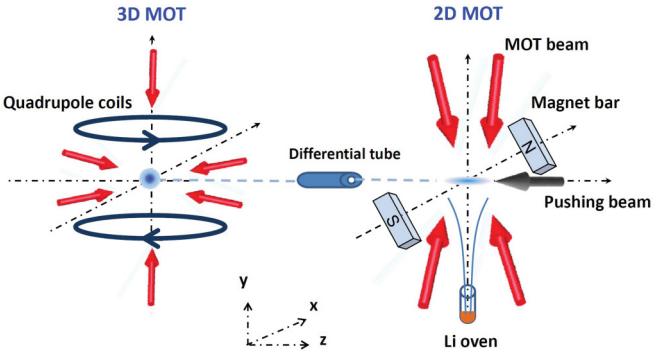

FIG. 1. (Color online) Schematic of the experimental setup. The system consists of two cooling and trapping regions, the 2D MOT and 3D MOT. The initial fast-moving atoms are emitted from a baked lithium oven which is located 170 mm below from the center of the 2D MOT. Atoms cooled in the 2D MOT are extracted toward the 3D MOT by using a pushing beam. The cooling light in the 2D MOT has multiple frequency sidebands, which has a spectral width of 102 MHz to increase the capture velocity. Trapped atoms are detected in the 3D MOT using the fluorescence imaging method. The solid red arrows show the cooling laser beams for 2D and 3D MOTs, and the black solid arrow indicates the pushing beam.

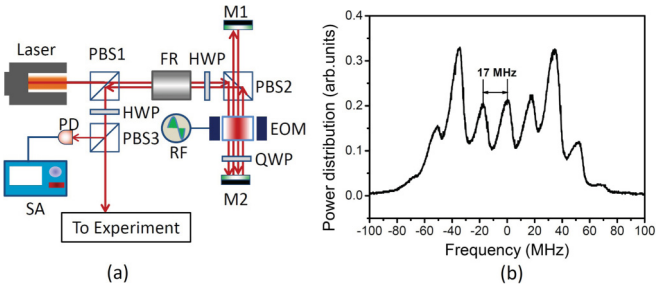

FIG. 2. (Color online) Generation of multiple sidebands. (a) Optical arrangement. PBS: polarization beam splitter; FR: Farady optical rotator; HWP: half-wave plate; QWP: quarter-wave plate; M1 and M2: mirrors; EOM: electro-optical modulator; RF: radio-frequency signal; PD: photodetector; SA: spectrum analyzer. (b) Power distribution of the multiple frequency components, which is recorded with a SA.

atom number is a good starting point to realize the quantum degeneracy. We finally analyze the loss due to fine-structure changing collisions and explain why the multiple-sideband cooling is successful for lithium. The method demonstrated in this paper has a potential to be widely used due to the simplicity of the experimental setup and big number of trapped atoms.

The paper is organized as follows. We first present our experimental setup in Sec. II. Then we show the experimental results and discuss them in Sec. III. Finally, the conclusions are summarized in Sec. IV.

II. EXPERIMENTAL SETUP

The experimental setup is sketched in Fig. 1. The vacuum system consists of two stainless chambers for 2D and 3D MOTs, respectively. As the hyperfine splitting of the excited ($2P_{3/2}$) state of ^{6}Li is much smaller than the corresponding natural linewidth ($\Gamma = 2\pi \times 5.87$ MHz), the cooling and repumping light should have comparable powers. These two laser frequencies (different from each other by the hyperfine splitting of the ground $2S_{1/2}$ state, $\Delta = 2\pi \times 228$ MHz) should be amplified separately. The reason is that simultaneous amplification of the two components with a small frequency difference in a taped amplifier (TA) will decrease the number of trapped atoms, which follows from our previous work [26]. With these arguments, the output of an external cavity diode laser (Topitca DL100@671nm 18 mW) is power amplified in a TA chip and then equally divided into two beams. After passing through a series of acousto-optical modulators (AOMs) the two beams have the frequency difference equal to the hyperfine splitting of the ground state. Then they are separately power amplified using two other TA chips, which allows us to have high powers for optical cooling and repumping, respectively. The laser frequency is locked onto the atomic transition line using the Doppler-free saturated absorption spectroscopy in a lithium heat pipe. In the 2D MOT, the cooling and repumping light get together and cool atoms in the x-y plane. The line quadrupole magnetic field is supplied by two sets of $Nd_2Fe_{14}B$ magnet bars (labeled with N and S) placed at the x axis, where the axial magnetic field is uniform and the radial magnetic gradient can be modulated by changing the number of the magnet bars. The lithium oven (containing a mixture of 4 g enriched ^{6}Li with an abundance of 95% and 2 g natural lithium) is connected to the main chamber using a stainless tube below the 2D MOT, with a diameter of 16 mm and a length of 170 mm. Being heated to about 600 K, fast-moving atoms are emitted from the oven upward, where the motion in the x-y plane is slowed in the 2D MOT region. A differential tube with a diameter of 3 mm and a length of 50 mm is placed between the two MOTs, which decreases the vacuum pressure in the 3D MOT by two orders of magnitude. The cooled atoms in the 2D MOT are pushed to the 3D MOT using a resonant beam with a power of 1 mW, and then the trapped atoms are detected using the fluorescence imaging method.

To improve the lithium loading, we broaden the spectral width of the cooling laser in the 2D MOT by generating multiple frequency sidebands with a small separation. We modulate the light phase in an electro-optical modulator (EOM) as shown in Fig. 2(a). Considering that only the horizontally polarized light can be phase-modulated by a rf signal in the EOM, we arrange the light to pass through the EOM four times and twice it has a horizontal linear polarization. Multiple sidebands are produced due to the nonlinearity effect in the EOM [24] and the output beam is spatially separated from the input. For detecting the distribution of these sidebands we use the heterodyne measurement to analyze the frequency-beat signal between the sidebands and an additional reference beam [not shown in Fig. 2(a)] [24,26,27]. This beam has a frequency separated by about 300 MHz from that of the cooling light. The frequency beat signal is then recorded by a spectrum analyzer. By choosing an optimal rf power we can get six sidebands and a carrier frequency as shown in Fig. 2(b), where the total power is almost equally distributed among the seven components. The spectral width is 102 MHz under a rf driving signal with a frequency of 17 MHz. We also modulate the repumping light with a 12 MHz rf signal and get a spectral width of 72 MHz. In the following discussion

we only include the sideband effect of the cooling light for simplicity.

III. EXPERIMENTAL RESULTS AND DISCUSSION

Atoms with velocities lower than the capture velocity v_c are sufficiently slowed down after entering the region of the intersecting laser beams, and then they can be loaded into a MOT. So, the capture velocity v_c plays an important role in determining the atom trapping efficiency. Solving the steady-state rate equation $\partial N/\partial t = R - \Gamma_c N = 0$, the number of trapped atoms can be written as [28,29]

$$N = \frac{R}{\Gamma_c} = 0.1\frac{A}{\sigma}\left(\frac{v_c}{v_{th}}\right)^4, \tag{1}$$

where R is the capture rate, Γ_c is the rate of collisions of trapped atoms with atoms of the background gas, $\sigma = 4.4 \times 10^{-14}$ cm^2 [25] is the total cross section for these collisions, $A = \pi d^2$ is the trap surface with d being the diameter of the laser beam, and v_{th} is the average velocity of the background gas atoms. This calculation neglects the contribution of intratrap collisions to the loss rate in the trap. For the densities of background vapor and trapped atoms at which we operate, this contribution is relatively small. In calculating the capture velocity v_c, we only compute the one-dimensional slowing force acting on atoms in the trapping region because this force is nearly the same along all three axes. For simplicity, we treat the atom as a two-level system and ignore effects of the magnetic field and the Gaussian intensity profile of laser beams. Then we can write the radiation-pressure force for the single-frequency cooling in the form

$$F = \frac{\hbar k\Gamma}{2}\left[\frac{I/I_s}{1 + I/I_s + \left(\frac{2(\Delta_0 - kv)}{\Gamma}\right)^2} - \frac{I/I_s}{1 + I/I_s + \left(\frac{2(\Delta_0 + kv)}{\Gamma}\right)^2}\right]. \tag{2}$$

For the multiple-sideband cooling we have

$$F = \frac{\hbar k\Gamma}{2}\sum_{i=1}^{7}\left[\frac{I/I_s}{1 + I/I_s + \left(\frac{2(\Delta_i - kv)}{\Gamma}\right)^2} - \frac{I/I_s}{1 + I/I_s + \left(\frac{2(\Delta_i + kv)}{\Gamma}\right)^2}\right], \tag{3}$$

where $k = 9.36 \times 10^4$ cm^{-1} is the wave number of the cooling light, $\Gamma = 2\pi \times 5.87$ MHz is the linewidth of the excited state, I is the intensity of each beam, and $I_s = 2.54$ mW/cm^2 is the saturation intensity. The quantity Δ_0 is the laser detuning from the resonant transition in the single frequency cooling. In the multiple-sideband cooling, Δ_4 is the laser detuning of the carrier frequency, and $\Delta_i = \Delta_4 + (i-4) \times q$, where $q = 2\pi \times 17$ MHz is the frequency separation between two adjacent components. There are in total seven frequency components, which means that $i = 1,2,\ldots,7$. An atom with an initial velocity v_c will be captured in the 3D MOT with the help of the pushing beam if its velocity is reduced to zero by the scattering force during the flight through the 2D MOT beams. By numerically solving Eqs. (2) and (3) we can calculate the capture velocities as functions of the cooling light intensity. The results are shown in Fig. 3. In the multiple-sideband cooling we assume for simplicity that the total power distributes equally among the seven frequency components. It is obvious that the capture velocity in the multiple-sideband cooling is dramatically increased compared to that in the single-frequency cooling. For example, when the cooling light power is 1.9 mW/cm^2 the capture velocity in the multiple-frequency cooling is 74.7 m/s, while it is 47.8 m/s in the single-frequency cooling.

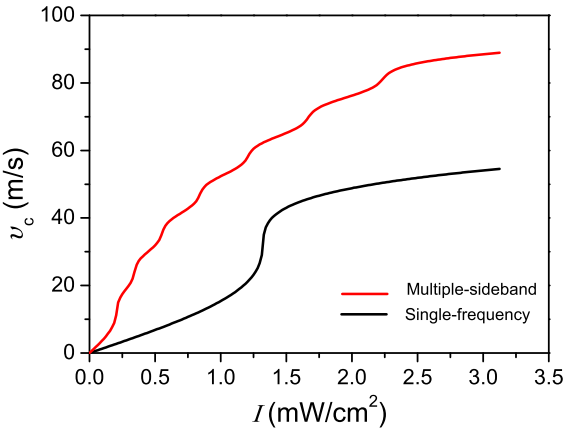

FIG. 3. (Color online) Capture velocity vs the cooling light intensity per beam in the 2D MOT ($d = 4$ cm, $\Delta_0 = -8.2\Gamma$, and $\Delta_4 = -11.9\Gamma$). Both detunings are close to the optimal values for achieving the maximum atom number as shown in Fig. 4. The red curve indicates v_c for the multiple-sideband cooling, and the black curve for the single-frequency cooling.

Compared to the single-frequency cooling, the advantage of the multiple-sideband cooling is that it can slow faster atoms and thus increase the atom trapping efficiency. In laser cooling it is required to keep the cooling light frequency resonant with moving atoms, including the Doppler shift. Thus, exploring the dependence of the atom trapping efficiency on the laser detuning (Δ_0 or Δ_4), one can demonstrate the preference of the multiple-sideband cooling. In the experiment, it is difficult to directly measure the capture velocity, while probing the number of trapped atoms is easy. We probe the number of trapped atoms in the 3D MOT once they are pushed there from the 2D MOT. To compare the atom trapping efficiency in the single-frequency cooling with that in the multiple-sideband one, we fix all experimental parameters the same except frequency components in the cooling light. We scan the cooling light detuning in the 2D MOT with the help of a AOM in the double-pass configuration and detect the number of trapped number using the fluorescence imaging method with a digital CCD. The results are shown in Fig. 4. In the multiple-sideband cooling, the theoretical prediction for the atom number has been multiplied by 2.5 to match the experimental data, while the multiplying factor in the single frequency cooling is 4.6 which is close to 3.3 in Ref. [28]. The underestimation of the theoretical prediction mainly comes from two aspects: (i) we neglect the effect of the magnetic field which may increase the atomic trapping efficiency [28]; (ii) when cooled atoms in the 2D MOT are pushed to the 3D MOT, the 2D MOT can cool fast-moving atoms again. We do not include this reloading

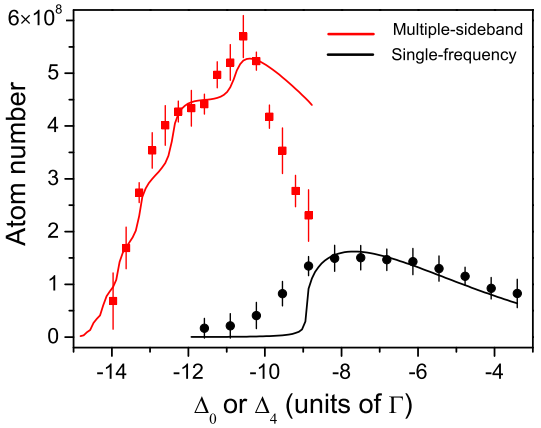

FIG. 4. (Color online) Number of trapped atoms in the 3D MOT vs the cooling light frequency detuning in the 2D MOT (Δ_0 for the single-frequency cooling and Δ_4 for the multiple-sideband cooling). In the 2D MOT we have $d = 4$ cm, $I = 1.9$ mW/cm^2, and $\partial B/\partial x = \partial B/\partial y = 50$ G/cm. In the 3D MOT the parameters are $d = 3$ cm, $I = 2.0$ mW/cm^2, and $\partial B/\partial x = \partial B/\partial z = 7$ G/cm. Red squares and black circles show experimental results for the multiple-sideband and single-frequency cooling, respectively. Each experimental point comes from five measurements and the error bars indicate the standard deviation (SD). Solid red and black curves are theoretical predictions from Eqs. (3) and (2), respectively.

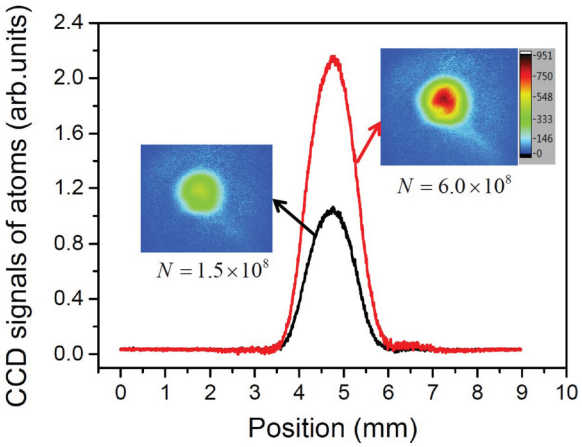

FIG. 5. (Color online) Fluorescence images of trapped atoms in the 3D MOT. The red and black solid curves are the 1D integrated fluorescence for the multiple-sideband and single-frequency cooling, respectively. The 2D fluorescence images are also inserted in the plot. In the multiple-sideband cooling $N = 6.0 \times 10^8$ and in the single-frequency cooling $N = 1.5 \times 10^8$. The color in the 2D images is scaled to the fluorescence amplitude on the CCD.

process. The simple model based on a two-level system qualitatively agrees with the experimental data, predicting the main trend of the variation of the atom number versus the laser detuning. The optimal detuning ($\Delta_4 = -10.6\Gamma$) for getting the maximum atom number in the multiple-sideband cooling is much bigger than that in the single-frequency cooling ($\Delta_0 = -7.5\Gamma$), which indicates that faster-moving atoms can be slowed in our proposed scheme. The maximum number of trapped atoms in the multiple-sideband cooling is $5.7(0.4) \times 10^8$. It has been increased by a factor of 3.8 compared to that in the single-frequency cooling.

In the multiple-sideband cooling, both theoretical predictions and experimental results show a steplike increase in the number of trapped atoms when the laser detuning is reduced towards the optimal value. This phenomenon is also shown in Ref. [24] and in Fig. 3. The steplike behavior results from the discrete distribution of the seven frequency components with a $2\pi \times 17$ MHz separation. Our calculation shows that this behavior will become less and less visible when decreasing the frequency separation. In addition, when Δ_4 is close to $-2\pi \times 51$ MHz and thus the sideband (denoted by Δ_7) becomes nearly resonant with the atomic transition, the loss due to light-assisted collisions will grow. Our calculation does not include this loss. This may explain why in the multiple-sideband cooling the experimental results decrease more rapidly than the theoretical prediction in the small-detuning region as shown in Fig. 4. From our calculation the capture velocity can become negative when $|\Delta_4| < 2\pi \times 51$ MHz, meaning that the photon scattering force will accelerate atoms. In this condition Eq. (1) will no longer be valid to predict the number of trapped atoms.

We also optimize the magnetic field gradient and the laser detuning in the 2D MOT to get the maximum number of trapped atoms in the 3D MOT, while other parameters are kept the same as in Fig. 4. The fluorescence images of trapped atoms are shown in Fig. 5 and the corresponding experimental parameters are given in Table I. The atom number in Fig. 5 is from one measurement, while in Table I it is the average over five measurements. In the multiple-sideband cooling the number of trapped atoms in the 3D MOT is 6.0×10^8, which is an increase by a factor of 4 compared to that in the single-frequency cooling, while in Ref. [24] this factor is 3.1. The enhancement of the atom number is a good starting point to realize the quantum degeneracy. The central point and width of the distribution of trapped atoms for these two kinds of cooling is almost the same within ± 30 μm, and it mainly results from the same parameters in the 3D MOT [27].

The number of atoms loaded into the trap depends not only on the loading process, but also on the loss in which atoms are ejected from the trap. The presence of nearly resonant, red-detuned light will produce fine-structure changing collisions by inducing transitions to excited molecular states [30]. So, the multiple-sideband cooling can enhance the capture velocity by

TABLE I. Experimental parameters in the 2D MOT for achieving the maximum number of trapped atoms in the 3D MOT. The quantity q is the separation between two adjacent frequency components, No is the number of sidebands in the 2D MOT, and N is the atom number in the 3D MOT.

Parameters	Single frequency	Multiple sideband
Cooling detuning (Γ)	−7.5	−10.9
Cooling q (MHz)		$2\pi \times 17.0$
Cooling No		6
Repumping detuning (Γ)	−2.4	−6.8
Repumping q (MHz)		$2\pi \times 12.0$
Repumping No		6
$\partial B/\partial x$ (G/cm)	50.0	45.0
N ($\times 10^8$)	1.5(0.5)	6.1(0.9)

TABLE II. Resulting velocity due to fine-structure changing collisions for different alkali-metal atoms.

	^{6}Li	^{23}Na	^{40}K	^{87}Rb	^{133}Cs
Δ_{FS} (THz)	0.0101	0.5162	1.7301	7.1230	16.6097
v_{FS} (m/s)	26.0	94.9	131.7	181.2	223.8

coupling faster atoms, but on the other hand it will increase the loss due to fine-structure changing collisions. Assuming that atoms are nearly at rest before collisions we can calculate the resulting velocity due to the fine-structure changing collision, $2\pi \times \hbar\Delta_{FS} = 2mv_{FS}^2/2$ with Δ_{FS} being the fine-structure splitting. The results are shown in Table II for different alkali-metal atoms. For each kind of atom we only calculate v_{FS} for one isotope. The velocity v_{FS} has almost the same value for different isotopes of the same atom because of the similar fine-structure splitting and atomic mass. Due to its small fine-structure splitting (∼10 GHz), v_{FS} of lithium is much smaller than the capture velocity with a common cooling light intensity as shown in Fig. 3. So, after fine-structure changing collisions lithium atoms can be recaptured in the multiple-sideband cooling. For sodium v_{FS} is 94.9 m/s and it may be smaller than the capture velocity in the multiple-sideband cooling. Previously, Zhu and colleagues have cooled sodium atoms using the broadband-laser cooling which is similar to the multiple-sideband cooling [31]. For potassium, rubidium, and cesium, v_{FS} is quite big, far beyond experimental conditions for the multiple-sideband cooling with a common laser power. This may explain the failure of earlier efforts to trap cesium with the broadband or multiple-sideband cooling [28,29]. If one puts an atomic block in the central area of the laser beam to produce a region without sideband-induced loss [23,24,32], the multiple-sideband cooling may be available for these heavier atoms.

IV. CONCLUSION

In conclusion, we experimentally and theoretically demonstrate the enhancement of lithium trapping efficiency in the 3D MOT by using the multiple-sideband cooling in the 2D MOT. The number of trapped atoms is higher by a factor of 4 than in the case of the single-frequency cooling. The dependence of the atom number on the cooling light detuning has been investigated, and our experimental results have a good agreement with the prediction based on a simple two-level model. We also analyze the loss due to fine-structure changing collisions and explain why the multiple-sideband cooling is efficient for lithium. The method demonstrated in this paper has a potential to be widely used due to the simplicity of the experimental setup and big number of trapped atoms.

ACKNOWLEDGMENTS

We thank G. V. Shlyapnikov for helpful comments. This work is supported by NSFC (Grants No. 11434015, No. 91336106, No. 11204355, No. 11474315, and No. 11004224), NBRP-China (Grant No. 2011CB921601), and programs in Hubei province (Grant No. 2013CFA056).

[1] W. D. Phillips and H. Metcalf, Laser deceleration of an atomic beam, Phys. Rev. Lett. **48**, 596 (1982).
[2] H. J. Metcalf and P. van der Straten, *Laser Cooling and Trapping* (Springer, New York, 1999).
[3] M. Kasevich and S. Chu, Atomic interferometry using stimulated Raman transitions, Phys. Rev. Lett. **67**, 181 (1991).
[4] B. J. Bloom, T. L. Nicholson, J. R. Williams, S. L. Campbell, M. Bishof, X. Zhang, W. Zhang, S. L. Bromley, and J. Ye, An optical lattice clock with accuracy and stability at the 10^{-18} level, Nature (London) **506**, 71 (2014).
[5] N. Hinkley, J. A. Sherman, N. B. Phillips, M. Schioppo, N. D. Lemke, K. Beloy, M. Pizzocaro, C. W. Oates, and A. D. Ludlow, An atomic clock with 10^{-18} instability, Science **341**, 1215 (2013).
[6] M. McDonald, B. H. McGuyer, G. Z. Iwata, and T. Zelevinsky, Thermometry via light shifts in optical lattices, Phys. Rev. Lett. **114**, 023001 (2015).
[7] I. Bloch, J. Dalibard, and W. Zwerger, Many-body physics with ultracold gases, Rev. Mod. Phys. **80**, 885 (2008).
[8] D. S. Jin and J. Ye, Introduction to ultracold molecules: New frontiers in quantum and chemical physics, Chem. Rev. **112**, 4801 (2012).
[9] M. H. G. de Miranda, A. Chotia, B. Neyenhuis, D. Wang, G. Quéméner, S. Ospelkaus, J. L. Bohn, J. Ye, and D. S. Jin, Controlling the quantum stereodynamics of ultracold bimolecular reactions, Nat. Phys. **7**, 502 (2011).
[10] C. Chin, R. Grimm, P. Julienne, and E. Tiesinga, Feshbach resonances in ultracold gases, Rev. Mod. Phys. **82**, 1225 (2010).
[11] M. Horikoshi, S. Nakajima, M. Ueda, and T. Mukaiyama, Measurement of universal thermodynamic functions for a unitary Fermi gas, Science **327**, 442 (2010).
[12] S. Nascimbene, N. Navon, K. J. Jiang, F. Chevy, and C. Salomon, Exploring the thermodynamics of a universal Fermi gas, Nature (London) **463**, 1057 (2010).
[13] A. Schirotzek, C. H. Wu, A. Sommer, and M. W. Zwierlein, Observation of Fermi polarons in a tunable Fermi liquid of ultracold atoms, Phys. Rev. Lett. **102**, 230402 (2009).
[14] S. Nascimbene, N. Navon, K. J. Jiang, L. Tarruell, M. Teichmann, J. McKeever, F. Chevy, and C. Salomon, Collective oscillations of an imbalanced Fermi gas: Axial compression modes and polaron effective mass, Phys. Rev. Lett. **103**, 170402 (2009).
[15] Y. J. Lin, K. Jimenez-Garcia, and I. B. Spielman, Spin-orbit-coupled Bose-Einstein condensates, Nature (London) **471**, 83 (2011).
[16] S-G. Peng, X-J. Liu, H. Hu, and K. J. Jiang, Momentum-resolved radio-frequency spectroscopy of a spin-orbit-coupled atomic Fermi gas near a Feshbach resonance in harmonic traps, Phys. Rev. A **86**, 063610 (2012).
[17] K. Gunter, T. Stoferle, H. Moritz, M. Kohl, and T. Esslinger, p-wave interactions in low-dimensional fermionic gases, Phys. Rev. Lett. **95**, 230401 (2005).

[18] S-G. Peng, S. Tan, and K. J. Jiang, Manipulation of p-wave scattering of cold atoms in low dimensions using the magnetic field vector, Phys. Rev. Lett. **112**, 250401 (2014).

[19] M. Bartenstein, A. Altmeyer, S. Riedl, R. Geursen, S. Jochim, C. Chin, J. H. Denschlag, R. Grimm, A. Simoni, E. Tiesinga, C. J. Williams, and P. S. Julienne, Precise determination of ^{6}Li cold collision parameters by radio-frequency spectroscopy on weakly bound molecules, Phys. Rev. Lett. **94**, 103201 (2005).

[20] A. Ridinger, S. Chaudhuri, T. Salez, U. Eismann, D. R. Fernandes, K. Magalhaes, D. Wilkowski, C. Salomon, and F. Chevy, Large atom number dual-species magneto-optical trap for fermionic ^{6}Li and ^{40}K atoms, Eur. Phys. J. D **65**, 223 (2011).

[21] Z. Lin, K. Shimizu, M. Zhan, F. Shimizu, and H. Takuma, Laser cooling and trapping of Li, Jpn. J. Appl. Phys. **30**, L1324 (1991).

[22] C. C. Bradley, J. G. Story, J. J. Tollett, J. Chen, N. W. M. Ritchie, and R. G. Hulet, Laser cooling of lithium using relay chirp cooling, Opt. Lett. **17**, 349 (1992).

[23] W. Gunton, M. Semczuk, and K. W. Madison, Realization of BEC-BCS-crossover physics in a compact oven-loaded magneto-optic-trap apparatus, Phys. Rev. A **88**, 023624 (2013).

[24] B. P. Anderson and M. A. Kasevich, Enhanced loading of a magneto-optic trap from an atomic beam, Phys. Rev. A **50**, R3581 (1994).

[25] T. G. Tiecke, S. D. Gensemer, A. Ludewig, and J. T. M. Walraven, High-flux two-dimensional magneto-optical-trap source for cold lithium atoms, Phys. Rev. A **80**, 013409 (2009).

[26] H. Luo, K. Li, D. Zhang, T. Gao, and K. J. Jiang, Multiple side-band generation for two-frequency components injected into a tapered amplifier, Opt. Lett. **38**, 1161 (2013).

[27] J. L. Booth, J. V. Dongen, P. Lebel, B. G. Klappauf, and K. W. Madison, Dual-channel amplification in a single-mode diode laser for multi-isotope laser cooling, J. Opt. Soc. Am. B **24**, 2914 (2007).

[28] K. Lindquist, M. Stephens, and C. Wieman, Experimental and theoretical study of the vapor-cell Zeeman optical trap, Phys. Rev. A **46**, 4082 (1992).

[29] K. E. Gibble, S. Kasapi, and S. Chu, Improved magneto-optic trapping in a vapor cell, Opt. Lett. **17**, 526 (1992).

[30] A. M. Smith, K. Burnett, and P. S. Julienne, Semiclassical theory of collision-induced loss from optical traps, Phys. Rev. A **46**, 4091 (1992).

[31] M. Zhu, C. W. Oates, and J. L. Hall, Continuous high-flux monovelocity atomic beam based on a broadband laser-cooling technique, Phys. Rev. Lett. **67**, 46 (1991).

[32] K. Ladouceur, B. G. Klappauf, J. V. Dongen, N. Rauhut, B. Schuster, A. K. Mills, D. J. Jones, and K. W. Madison, Compact laser cooling apparatus for simultaneous cooling of lithium and rubidium, J. Opt. Soc. Am. B **26**, 210 (2009).